Supporting Information

Baumgartner et al. 10.1073/pnas.1317176111

SI Text

Overview of Optical and Chemical Particulate Matter Exposure Measurements. All air pollution exposure samples were collected on Teflon filters and first analyzed for fine particulate matter ($PM_{2.5}$) mass and black carbon (BC). Portions of each filter were then used for chemical analysis to estimate water-soluble organic carbon (WSOC). We analyzed a subset of PM samples for nonpolar organic hopanes, which are specific markers of motor vehicle emissions in our study setting. More detail about these specific PM components and their measurement is described below.

BC. BC refers to the dark, light-absorbing components of aerosols that contain elemental carbon. Although BC and elemental carbon are often used to describe the same PM fractions, BC is an operationally defined term which describes carbon measured by light absorption. It is therefore different from elemental carbon which is usually measured using thermal–optical methods. BC is emitted from combustion processes, and primary sources include household use of biomass and coal fuels, combustion engines (especially diesel), heavy oil- or coal-fired power stations, and the field burning of agricultural wastes. In addition to climate warming, other regional climate impacts of BC may include increased glacial retreat and changes in precipitation patterns in Asia (1, 2). In health studies, BC is often used as a surrogate for traffic-related PM and has been more strongly associated with a range of cardiovascular and some respiratory outcomes than PM mass in studies conducted in the United States and Europe (3, 4).

Optical Measurement of BC Exposure. BC is defined as the fraction of carbonaceous aerosol absorbing light over a broad region of the visible spectrum. We estimated BC components of total PM mass based on reflectance analysis using an optical transmissometer data acquisition system (SootScan Model OT21; Magee Scientific). This system provides measurements that are highly correlated with concentrations measured using the National Institute for Occupational Safety and Health (NIOSH) thermal–optical method (5). The optical method used in our study both measures and compares the transmission intensity of light at 880 nm passing through an exposed Teflon filter with that of a blank, unexposed filter. The resulting light absorption (ATN) coefficient was computed based on the amount of light transmitted through the exposed filter (I) and the amount transmitted through the blank filter (I_0), where $ATN = 100\ln(I_0/I)$.

We determined BC density (micrograms per square centimeter) by dividing ATN by the specific attenuation coefficient σ_{ATN}, using the relationship, $BC = ATN/\sigma_{ATN}$ (6). BC density was converted to BC exposure concentration for women in our study using the total volume of air (cubic meters) that passed through the exposed Teflon filters during 24-h sampling periods. To account for underestimation of ATN at higher BC concentrations during reflectance analysis (7), we applied an empirical correction factor described elsewhere (8). The instrument was rezeroed with a blank filter between measurements. We obtained the final BC exposure estimate for each participant by averaging five replicate measurements conducted on each filter sample. BC was undetectable on all field blanks.

WSOC and Organic Tracers. Organic carbon can be emitted both from primary emission sources (e.g., biomass combustion, motor vehicles, and industrial sources) and from chemical reactions of gaseous organic precursors in the atmosphere (9). Particulate WSOC accounts for a large proportion of organic carbon in certain settings and may influence the Earth's radiative forcing by acting as cloud condensation nuclei (10). Biomass combustion is a primary source of WSOC in the atmosphere (11, 12). In the absence of emissions from biomass combustion, WSOC is often considered a proxy for secondary organic aerosols due to the highly oxidized nature of water-soluble organic aerosol species (13). Thus, whereas BC serves as a more direct marker of combustion PM, the water-soluble components of PM may be more specific to biomass combustion (14). For example, WSOC accounted for as much as 75% of total PM mass during prescribed biomass burning events in Amazonia (15, 16).

We focused our analysis of source tracers on nonpolar organic hopanes, which are compounds that are present in the lubricating oil of engines (17). Hopanes are relatively involatile and stable compounds that are present in the emissions from mobile sources, fuel oil combustion, and coal combustion (18). In our study site where there is very minimal or no coal or fuel oil combustion, hopanes are tracers for motor vehicle emissions and can be used to distinguish diesel and gasoline engine emissions from other sources of organic carbon (19). We focused our analysis on hopanes as they are more specific and robust markers of motor vehicle emissions than other molecular markers like steranes and polycyclic aromatic hydrocarbons.

To analyze samples and blanks for WSOC, we placed 1.5 cm^3 punches from the Tefon filters in capped conical glass flasks containing 12 mL purified water (Cascada IX; Pall Corp.). We agitated the flasks on a shaker table (120 rpm) at room temperature for 16-h (20, 21). Filter debris and suspended insoluble particles were removed from the water extracts using a polyethersulfone hydrophilic syringe filter (0.45-μm membrane). WSOC was measured with a Shimadzu TOC-V CSH/CSN Total Organic Carbon Analyzer (Shimadzu Corp.) using the nonpurgeable organic carbon method (22). Analytical precision for this method typically falls in the range of 1% to 4% relative SD. The reported WSOC exposures were obtained by averaging the results from three replicates for each filter. The limit of detection for the TOC-V_{CPH} is 4 μg/L and the SD of the repeated measurements is <1.5% (values provided by manufacturer). All exposure samples were laboratory and field blank subtracted to correct for WSOC contamination of filters, glassware, etc. Blank subtractions were conducted using the average of all field blanks [mean (SD) of blanks = 2.98 (0.71) μg]. Finally, WSOC exposure estimates were multiplied by 2.0 to yield water-soluble organic mass (WSOM) from biomass combustion for statistical analysis, according to Turpin and Lim (23) and Bae et al. (24).

The extraction and analysis methods to quantify individual organic compounds were based on established solvent extraction methods (25). We analyzed samples and blanks for three hopane compounds, specifically 17α(H)-22,29,30-trisnorhopane, 17α(H),21β(H)-hopane, and 17α(H),21β(H)-29-norhopane. Procedures for sample extraction and molecular quantification for the organic tracers are described elsewhere (25) and thus only a brief summary is presented here. The filter samples were spiked with known quantities of isotope-labeled internal standard compounds, then extracted for 15 min with dichloromethane and methanol using an ultrasonic bath. This procedure was repeated three times to ensure adequate recovery of organic carbon mass. The extract was transferred into a round-bottom flask (250 mL) and concentrated to 0.5mL using a rotary evaporator. Suspended particles were removed with a micro-syringe and filter, and the filtrate was collected in a centrifuge tube. To displace the solvent, 5 mL of dichloromethane was added into the centrifuge tube, and the mixture was evaporated to 0.5 mL under a gentle stream of nitrogen gas. We repeated this step twice.

Samples were analyzed using splitless autoinjection into a GC/MS system (GC model 6890 and MSD model 5975; Agilent) equipped with a 30 m × 0.25 mm × 0.25 μm fused-silica capillary column. Along with the samples, six dilutions of authentic quantification standard mixture solutions were also injected and used to build the calibrations curves for each compound. The precision of the spike and standards were used to estimate method precisions because duplicate samples were not available (26). Field blank concentrations of hopanes were below analytical detection limits.

Glassware used during chemical analysis was washed in the ultrasonic bath, rinsed with deionized water, and then baked at 550 °C for at least 6 h before use. The water was deionized and purified in a water purification system (Cascada IX; Pall Corp.). The standard mixture solutions used for calibration curves were obtained from University of Wisconsin-Madison.

Sensitivity Analyses Results. In our analysis comparing hopane exposure for women in the village closest to the highway vs. women in the village farthest from the highway, we excluded 17α(H),21β(H)-29-norhopane due to the large number of exposure samples falling below the limit of detection (n = 23 or 32%, of samples from women away from the highway; n = 5 or 13% of samples from women near the highway). For women whose exposure was below the limit of detection for the remaining two hopane compounds [n = 6 samples or 8% of total samples) for both 17α(H)-22,29,30-trisnorhopane and 17α(H),21β(H)-hopane], we estimated a 99% confidence interval (CI) for each compound's detection limit and then randomly assigned a concentration within this interval to each observation where the measured concentration was below the detection limit. Notably, of the 12 samples below the limit of detection, only one was from a woman in the village near the highway and the remaining samples were from women in the village farthest from the highway.

Geometric mean hopane exposure among women living near the highway was more than twice that of women living away from the highway (Table S4). In winter, geometric mean daily exposure among women near the highway was 6.0 ng/m^3 (95% CI, 4.1 to 8.8) compared with 3.0 ng/m^3 (95% CI, 2.1 to 4.3) for women away from the highway. In summer, average hopane exposure among women near the highway was just slightly lower (5.2 ng/m^3; 95% CI, 3.7 to 7.7) whereas exposure among women living away from the highway decreased considerably (1.9 ng/m^3 (95% CI, 0.9 to 4.0). Hopane exposure was higher in the winter for women in both villages. This may be due to a number of factors including varying environmental conditions (e.g., temperature and humidity) as well as seasonal differences in traffic levels or women's individual behavioral patterns.

As an additional sensitivity analysis, we evaluated the associations of systolic and diastolic blood pressure (SBP and DBP) with exposure to $PM_{2.5}$ mass, BC, and WSOM and expressed the results as the changes in blood pressure associated with a 1-interquartile range (IQR) increase in log-transformed pollutant exposure using one- and two-pollutant multivariate mixed-effects models. We conducted the same multivariate mixed-effects models as those reported in *Materials and Methods, Analysis*.

Supporting our findings in the main text, an IQR increase in ln (BC) exposure had the largest independent effect on both SBP and DBP (Fig. S2). In models with just one pollutant, an IQR increase in ln(BC) was the most strongly associated with higher SBP (3.6 mmHg; 95% CI, 2.0 to 5.2), followed by ln($PM_{2.5}$) (2.8 mmHg; 95% CI, 1.0 to 4.6) and ln(WSOM) (1.8 mmHg; 95% CI, 0.1 to 3.5). The estimated effect of BC on SBP was minimally affected by the inclusion of $PM_{2.5}$ mass or WSOM (<8% change) and it remained statistically significant after adjusting for other pollutants. In contrast, the estimated of $PM_{2.5}$ mass on SBP decreased by 71% and lost statistical significance when BC exposure was added to the model. WSOM had no effect on SBP after other pollutants were included in the model (Fig. S2*A*). We found similar results for DBP (Fig. S2*B*).

We also conducted a separate analysis for younger (25–50 y) vs. older women (>50 y) with the IQR in log-transformed pollution as our pollution measure. Supporting our findings in the main text, BC was more strongly associated with blood pressure than PM mass among both younger and older women. An IQR increase in ln(BC) exposure was associated with a 1.5-mmHg (95% CI, 0 to 3.0) higher SBP in younger women at the sample average, compared with 0.9 mmHg (95% CI, −0.9 to 2.7) for $PM_{2.5}$. Among women >50 y old, an IQR increase in ln(BC) exposure was associated with a 6.2-mmHg (95% CI, 3.4 to 9.0) higher SBP and a 2.4-mmHg (95% CI, 0.9 to 3.9) higher DBP compared with the 5.0-mmHg (95% CI, 1.9 to 8.1) higher SBP and 2.2-mmHg (95% CI, 0.5 to 3.9) higher DBP associated with an IQR increase in ln($PM_{2.5}$) exposure. In both age groups, the estimated effect of BC on blood pressure was minimally affected by the inclusion of $PM_{2.5}$ mass. In contrast, the estimated of $PM_{2.5}$ mass on blood pressure decreased considerably when BC was also included in the model (Fig. S3).

1. Menon S, Hansen J, Nazarenko L, Luo Y (2002) Climate effects of black carbon aerosols in China and India. *Science* 297(5590):2250–2253.
2. Qiu J, Yang L (2000) Variation characteristics of atmospheric aerosol optical depths and visibility in North China during 1980-1994. *Atmos Environ* 34:603–609.
3. United States Environmental Protection Agency (2012) Report to Congress on Black Carbon. Department of the Interior, Environment, and Related Agencies Appropriations Act, 2010 (Office of Air Quality Planning and Standards, Research Triangle Park, North Carolina), publication no. EPA-450/R-12-001.
4. Janssen NA, et al. (2011) Black carbon as an additional indicator of the adverse health effects of airborne particles compared with PM10 and PM2.5. *Environ Health Perspect* 119(12):1691–1699.
5. Ahmed T, et al. (2009) Measurement of black carbon (BC) by an optical method and a thermal-optical method: Intercomparison for four sites. *Atmos Environ* 43(40):6305–6311.
6. Hansen ADA, Rosen H, Novakov T (1984) The aethalometer—an instrument for the real-time measurement of optical absorption by aerosol particles. *Sci Total Environ* 36:191–196.
7. Bond TC, Covert DS, Müller T (2009) Truncation and angular-scattering corrections for absorbing aerosol in the TSI 3563 nephelometer. *Aerosol Sci Technol* 43(9):866–871.
8. Baumgartner J, et al. (2012) Household air pollution and children's blood pressure. *Epidemiology* 23(4):641–642.
9. Turpin BJ, Huntzicker JJ (1995) Identification of secondary organic aerosol episodes and quantitation of primary and secondary organic aerosol concentrations during SCAQS. *Atmos Environ* 29:3527–3544.
10. Saxena P, Hildemann LM, McMurry PH, Seinfeld JH (1995) Organics alter hygroscopic behavior of atmospheric particles. *J Geophys Res* 100:18755–18770.
11. Docherty KS, et al. (2008) Apportionment of primary and secondary organic aerosols in southern California during the 2005 study of organic aerosols in riverside (SOAR-1). *Environ Sci Technol* 42(20):7655–7662.
12. Park SS, Sim SY, Bae MS, Lee KY, Schauer JJ (2013) Investigation on size distributions of water-soluble components in particulate matter emissions from biomass burning. *Atmos Environ* 73:62–72.
13. Kanakidou M, et al. (2005) Organic aerosol and global climate modelling: A review. *Atmos Chem Phys* 5:1053–1123.
14. Sullivan AP, et al. (2006) Airborne measurements of carbonaceous aerosol soluble in water over northeastern United States: Method development and an investigation into water-soluble organic carbon sources. *J Geophys Res* 111(D23):16.
15. Graham B, et al. (2002) Water-soluble organic compounds in biomass burning aerosols over Amazonia-1. Characterization by NMR and GC-MS. *J Geophys Res* 107(D20):8047–8052.
16. Mayol-Bracero OL, et al. (2002) Water-soluble organic compounds in biomass burning aerosols over Amazonia-2. Apportionment of the chemical composition and importance of the polyacidic fraction. *J Geophys Res* 107(D20):8091–8102.
17. Rogge WF, Hildemann LM, Mazurek MA, Cass GR (1993) Sources of fine organic aerosol. II. Noncatalyst and catalyst-equipped automobiles and heavy-duty diesel trucks. *Environ Sci Technol* 27:636–651.
18. Zhang Y, et al. (2008) Characteristics of particulate carbon emissions from real-world Chinese coal combustion. *Environ Sci Technol* 42(14):5068–5073.
19. Schauer JJ, et al. (1996) Source apportionment of airborne particulate matter using organic compounds as tracers. *Atmos Environ* 30:3837–3855.
20. Zhang Y, Schauer JJ, Shafer MM, Hannigan MP, Dutton SJ (2008) Source apportionment of in vitro reactive oxygen species bioassay activity from atmospheric particulate matter. *Environ Sci Technol* 42(19):7502–7509.
21. Miller-Schulze JP, et al. (2011) Characteristics of fine particle carbonaceous aerosol at two remote sites in Central Asia. *Atmos Environ* 45(38):6955–6964.
22. Wangersky PJ (1993) Dissolved organic-carbon methods—A critical-review. *Mar Chem* 41:1–3.

23. Turpin BJ, Lim HJ (2001) Species contributions to PM2.5 mass concentrations: Revisiting common assumptions for estimating organic mass. *Aerosol Sci Technol* 35:602–610.
24. Bae MS, Schauer JJ, Turner JR (2006) Estimation of the monthly average ratios of organic mass to organic carbon for fine particulate matter at an urban site. *Aerosol Sci Technol* 40:1123–1139.
25. Zhang YX, Schauer JJ, Stone EA, Zhang YH, Shao M (2009) Harmonizing molecular marker analyses for organic aerosols. *Aerosol Sci Technol* 43:275–283.
26. Stone EA, et al. (2008) Source apportionment of fine organic aerosol in Mexico City during the MILAGRO experiment 2006. *Atmos Chem Phys* 8:1249–1259.

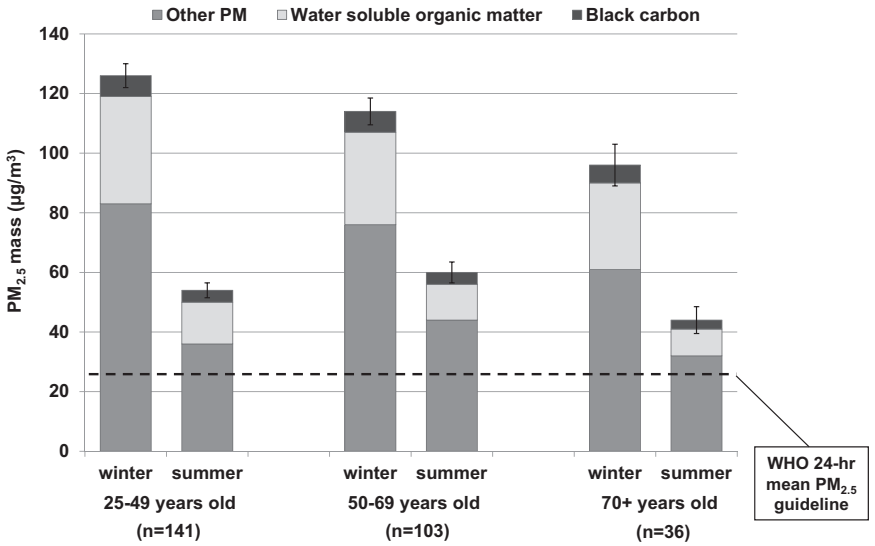

Fig. S1. Geometric mean daily personal exposure to $PM_{2.5}$ mass, BC, and WSOM (micrograms per cubic meter) in rural Chinese women, by season and age. The error bars indicate the 95% CIs for geometric mean $PM_{2.5}$ mass exposure. We used the three age groups presented in the figure because 50-y-old women may reduce their participation in agricultural work and spend more time at home, and 70-y-old women may also participate less often in household tasks like cooking. WHO, World Health Organization.

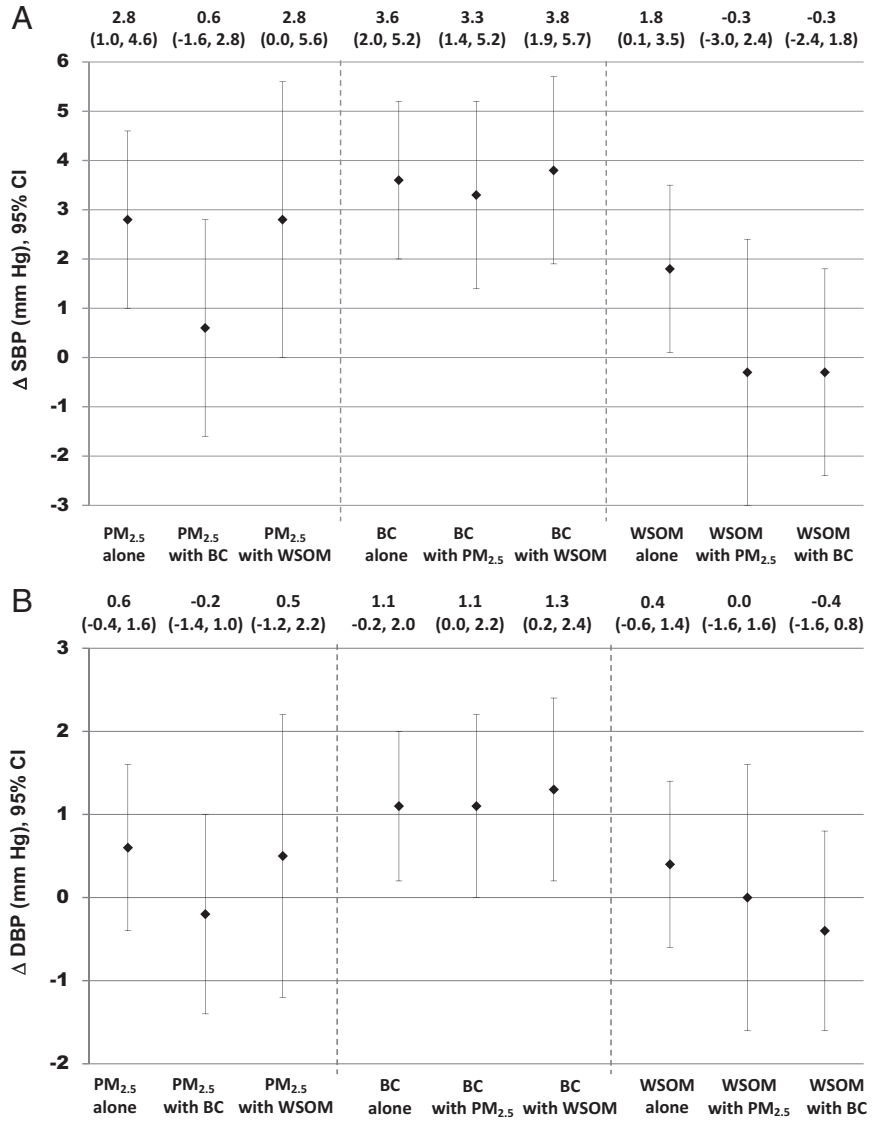

Fig. S2. Associations of IQR increases in log-transformed personal exposure to $PM_{2.5}$ mass, BC, and WSOM on (*A*) SBP and (*B*) DBP using one- and two-pollutant mixed-effects regression models. ΔSBP or ΔDBP represent the difference in SBP or DBP (with 95% CIs) associated with a 1-IQR increase in log-transformed pollutant exposure (equivalent to 44–148 μg/m^3 for $PM_{2.5}$, 3.3–7.4 μg/m^3 for BC, and 11–45 μg/m^3 for WSOM).

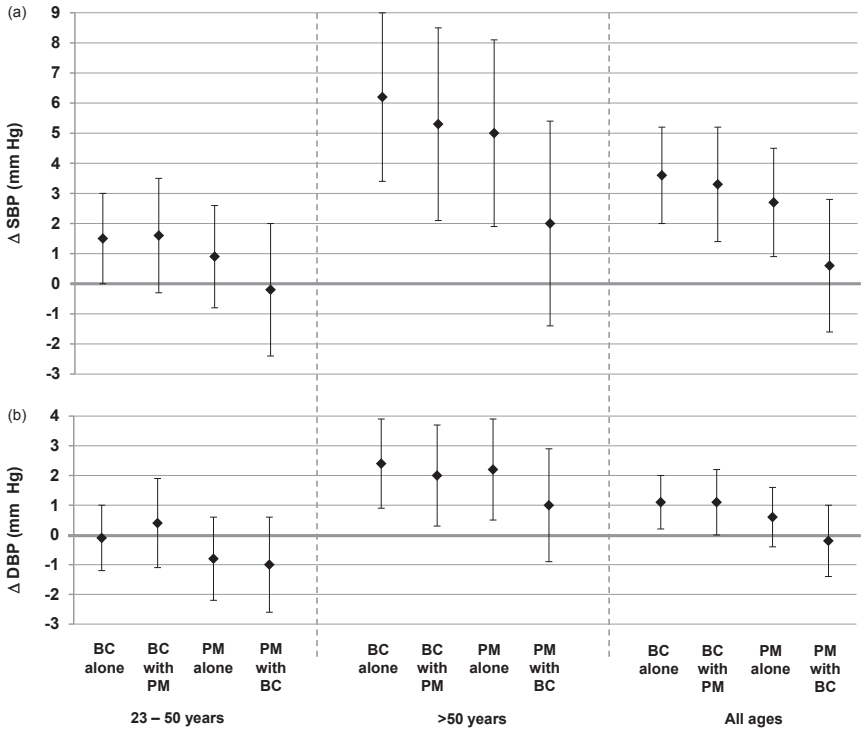

Fig. S3. Associations of IQR increases in log-transformed personal exposure to $PM_{2.5}$ mass and BC on (*A*) SBP and (*B*) DBP using one- and two-pollutant mixed-effects regression models, by age. ΔSBP or ΔDBP represent the difference in SBP or DBP (with 95% CIs) associated with a 1-IQR increase in log-transformed pollutant exposure (equivalent to 44–148 μg/m^3 for $PM_{2.5}$ and 3.3–7.4 μg/m^3 for BC).

Table S1. Demographic and health characteristics of study participants (n = 280)

Characteristic	Mean (SD)	Minimum–maximum
Age, y	51.9 (14.3)	25–90
Education, y	5.1 (3.3)	0–13
Waist circumference, cm	81.8 (9.1)	62–119
Body mass index, kg/m^2	22.6 (3.5)	15.6–36.1
Daily salt intake in cooked foods, g	5.6 (3.7)	3.1–26.5
Physical activity: daily no. of steps	7,450 (5,686)	290–41,881
Distance of home from the highway, m	248 (205)	9–1,342
SBP, mmHg	120.0 (19.9)	89.3–200.8
DBP, mmHg	72.4 (10.8)	50.0–116.8

Table S2. Health behaviors and existing cardiovascular conditions among study participants (n = 280)

Characteristic	No. (%)
Lives with at least one tobacco smoker	222 (80)
Hypertensive*	37 (13)
Currently taking antihypertensive medication	6 (2)
Physician-diagnosed diabetes	2 (<1)
Self-report of previous cardiovascular event	None

*Defined as SBP ≥ 140 mmHg and/or DBP ≥ 90 mmHg and/or current use of antihypertensive medication.

Table S3. Exposure correlation matrix for personal exposure to $PM_{2.5}$ mass and its components, by season

	Summer				Winter			
Pollutant	$PM_{2.5}$ mass	BC	WSOM	Hopanes*	$PM_{2.5}$ mass	BC	WSOM	Hopanes*
$PM_{2.5}$ mass	1.00				1.00			
BC	0.63	1.00			0.34	1.00		
WSOM	0.72	0.72	1.00		0.60	0.32	1.00	
Hopanes*	−0.65	−0.18	−0.38	1.00	−0.08	0.05	−0.18	1.00

PM, BC, and WSOM exposures are in micrograms per cubic meter, hopane exposure is in nanograms per cubic meter, and the results are for the Spearman rank correlations.
*Analysis of the correlation between hopanes and other pollutants is limited to the subsample of women in the village nearest to and farthest from the highway (n = 85 women).

Table S4. Geometric mean BC (μg/m^3) and hopane exposure (ng/m^3) in rural Chinese women, by season and distance from the highway

	Winter			Summer		
Pollutant	Near highway* GM (95% CI)	Away from highway GM (95% CI)	P value†	Near highway* GM (95% CI)	Away from highway GM (95% CI)	P value†
BC	6.9 (6.3 to 7.7)	5.8 (5.2 to 6.5)	0.01	3.7 (3.5 to 3.9)	4.0 (3.6 to 4.4)	0.15
Hopanes: total‡	6.0 (4.1 to 8.8)	3.0 (2.1 to 4.3)	0.01	5.2 (3.7 to 7.7)	1.9 (0.9 to 4.0)	0.02
17α(H)-22,29,30-trisnorhopane	2.7 (1.9 to 4.0)	0.8 (0.4 to 1.5)	0.02	1.8 (1.2 to 2.8)	0.5 (0.2 to 1.6)	0.28
17α(H),21β(H)-hopane	2.5 (1.2 to 5.4)	1.6 (1.0 to 2.5)	0.008	2.1 (2.2 to 4.5)	0.4 (0.1 to 1.6)	0.03

GM, geometric mean.
*For BC exposure (n = 280 women), near-highway exposure is for women in all study villages living in homes within the median distance from the highway (e.g., <208 m) and away-from-highway exposure is for women in homes farther than the median distance. For the subset of women with hopane exposure measurement (n = 85 women), near-highway refers to women living in the village closest to the highway (median distance = 76 m) and away-from-highway refers to women in the village farthest from the highway (median distance = 548 m).
†The statistical significance of the difference in geometric mean pollutant exposure between villages, under the null hypothesis that the geometric mean exposures of women in these groups are equal.
‡The sum of the two individual compounds reported here.